frontiers in Earth Science

ORIGINAL RESEARCH
published: 06 April 2021
doi: 10.3389/feart.2021.663574

Experimental Methods for the Quantitative Assessment of the Volume Fraction of Movable Shale Oil: A Case Study in the Jimsar Sag, Junggar Basin, China

Xia Luo, Zhongying Zhao*, Lianhua Hou*, Senhu Lin, Feifei Sun, Lijun Zhang and Yan Zhang*

Research Institute of Petroleum Exploration and Development, PetroChina, Beijing, China

OPEN ACCESS

Edited by:
Dongdong Wang, Shandong University of Science and Technology, China

Reviewed by:
Weilong Peng, SINOPEC Petroleum Exploration and Production Research Institute, China
Binfeng Cao, Institute of Geology and Geophysics (CAS), China

***Correspondence:**
Xia Luo
luoxia69@petrochina.com.cn
Zhongying Zhao
zhaozhongying@petrochina.com.cn
Lianhua Hou
houlh@petrochina.com.cn

Specialty section:
This article was submitted to Economic Geology, a section of the journal Frontiers in Earth Science

Received: *03 February 2021*
Accepted: *12 March 2021*
Published: *06 April 2021*

Citation:
Luo X, Zhao Z, Hou L, Lin S, Sun F, Zhang L and Zhang Y (2021) Experimental Methods for the Quantitative Assessment of the Volume Fraction of Movable Shale Oil: A Case Study in the Jimsar Sag, Junggar Basin, China. Front. Earth Sci. 9:663574. doi: 10.3389/feart.2021.663574

Deep insights into the movability of the retained shale oil are of great significance to shale oil. Rock and crude oil samples were collected from well J174 in the Jimsar Sag, Junggar Basin. Rock samples were subjected to different extraction followed by analysis of the component in the extracts, and measurement of porosity in conjunction with nuclear magnetic resonance and high-pressure mercury injection analysis. The results of these analyses were used to establish an experimental method for quantitative assessment of movable shale oil. The extract content of the component varied among different extraction and between mud shale and non-mud shale samples. The saturated hydrocarbon in the extracts of the mud shale was similar to those of the non-mud shale after extraction with $CHCl_3$ alone or after sequential extraction with $nC_6 + CHCl_3$. The aromatic hydrocarbon in the extract were significantly lower for the mud shale than for the non-mud shale after extraction with nC_6, but the opposite was observed after sequential extraction with $nC_6 + CHCl_3$. The contents of the non-hydrocarbon in the extract were significantly lower for the mud shale than for the non-mud shale after extraction with nC_6, but the opposite was observed after extraction with $CHCl_3$ or $nC_6 + CHCl_3$. The contents of the asphaltene in the extract were not significantly different for the mud shale and non-mud shale after extraction with nC_6, but the contents were higher for the mud shale than for the non-mud shale after extraction with $nC_6 + CHCl_3$ or $CHCl_3$. The viscosity of the crude oil was negatively correlated with the saturated hydrocarbon, was positively correlated with the aromatic hydrocarbon and non-hydrocarbon, and was not correlated with the asphaltene. For the mud shale and non-mud shale, their porosity after extraction with nC_6 or $CHCl_3$ was higher than their original porosity. Moreover, their porosity after extraction with $CHCl_3$ was higher than after extraction with nC_6. The movable oil was significantly correlated with the lithology, with sandstone allowing for a higher fluid movability than mud shale and dolomite allowing for a higher fluid movability than siliceous rocks.

Keywords: shale oil, volume fraction of movable oil, retained oil, sequential extraction, Jimsar Sag

INTRODUCTION

Shale oil has drawn a great deal of attention in terms of the global exploration and production of unconventional oil and gas (Goodarzi, 2020; Kim and Shin, 2020; Solarin, 2020; Kara and Isik, 2021). China's terrestrial shale oil has a huge resource potential, and breakthroughs have been achieved in the Permian Lucaogou Formation in the Jimsar Sag, Junggar Basin, as well as in the Chang 7 Member in the Ordos Basin (Hou et al., 2020a,b, 2021; Hu et al., 2020; Ma et al., 2020; Zhao et al., 2020). However, the shale oil is only in its initial stage and is under geological conditions that are dramatically different from those of the marine shale oil in North America. Chinese shale oil is mainly distributed in Mesozoic-Cenozoic shale strata, where the lacustrine mud shale is characterized by a low thermal maturity, with *Ro* values primarily ranging from 0.5 to 1.2%. The high stratigraphic heterogeneity, high oil density, and low oil fluidity pose significant challenges in the exploration and production of such shale oil. Therefore, it is extremely important to obtain a comprehensive, in-depth understanding of the movability of the retained oil in shale (Liu et al., 2012; Tao et al., 2012; Li et al., 2015; Xie et al., 2015). In this study, core samples of different lithologies were collected from the different strata in well J174 in the Jimsar Sag, Junggar Basin, and then, the samples were subjected to different extraction treatments with n-hexane (nC_6) and chloroform ($CHCl_3$), followed by porosity measurements to explore how the extract composition of the component and the rock porosity vary with the extraction treatments and rock types. Moreover, the volume fraction of the movable oil in the different lithologies was addressed from different aspects via nuclear magnetic resonance (NMR) analysis and high-pressure mercury injection analysis of representative rock samples.

SAMPLES AND METHODS

Rock and crude oil samples were collected from well J174 in the Jimsar Sag, Junggar Basin. The main crude oil production depths in well J174 are 3246–3285 m, at which the main lithology is characterized by the frequent interbedding of dolomitic siltstone with thin dolomitic shale. The rock samples were divided into mud shale samples and non-mud shale samples. The mud shale samples were mainly siliceous and dolomitic, while the non-mud shale samples were mainly muddy siltstone, dolomitic siltstone, and dolomite.

Rock cores were obtained through drilling, while the other samples were broken (120 mesh) for basic geological analysis (**Appendix Table A1**). The cores were separately subjected to single-solvent extraction with nC_6, single-solvent extraction with $CHCl_3$, and sequential extraction with nC_6 + $CHCl_3$. The porosity and permeability were measured by the helium method (Burnham, 2017; Gao and Li, 2018; Dong and Harris, 2020). The extraction steps were completed in the North China Oilfield Research Institute of the China National Petroleum Corporation (CNPC), while the rock porosity and permeability were determined in the Key Laboratory of Natural Gas Formation and Development of CNPC. The powdered samples were divided into two parts. (1) One part was extracted using only $CHCl_3$, and the extract was subjected to component-group isolation and quantification. (2) The other part was extracted using nC_6 and $CHCl_3$ in sequence, followed by component-group isolation and quantification for each solvent extract. All of the extraction experiments were conducted at Yangtze University. Representative lithological samples were selected for thermal dissolution followed by NMR and high-pressure mercury injection analysis in the Key Laboratory of Natural Gas Formation and Development of CNPC.

RESULTS AND DISCUSSION

Different Extraction Treatments

The powdered samples were either first extracted using nC_6 and then $CHCl_3$ or using only $CHCl_3$. The contents of the saturated hydrocarbon, the aromatic hydrocarbon, the asphaltene, and the non-hydrocarbon in each extract were determined. The experimental results are presented in **Appendix Table A2**. The cores were extracted using only nC_6 or only $CHCl_3$, followed by porosity and permeability measurements. The experimental results are also presented in **Appendix Table A2**. Five samples (#3, #9, #15, #16, and #22) were selected for NMR analysis,

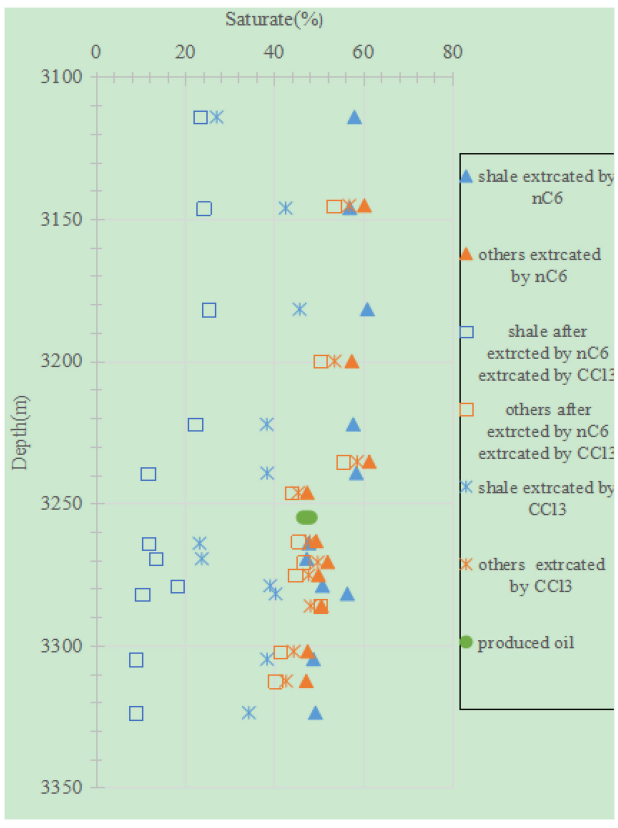

FIGURE 1 | Depth profile of the extract contents of the saturated hydrocarbon from the mud shale versus the non-mud shale after the different extraction treatments.

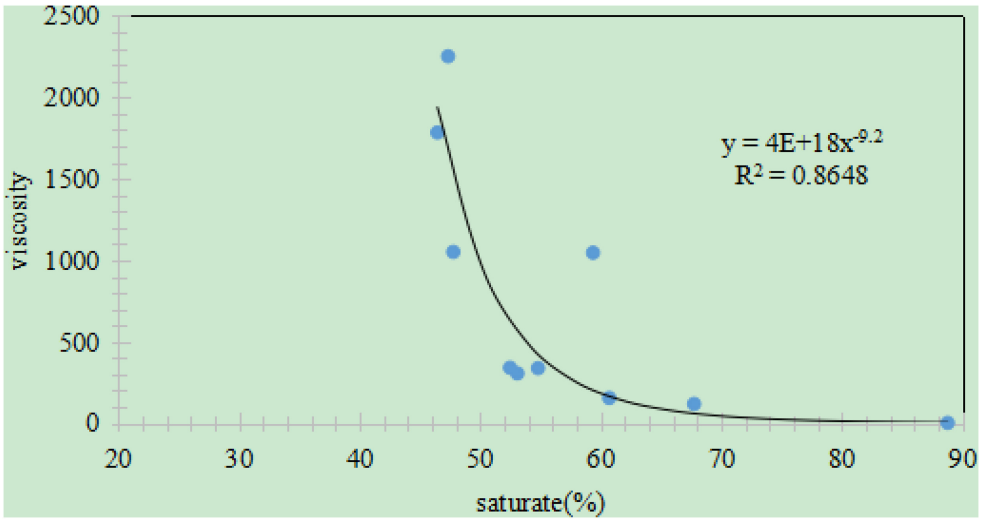

FIGURE 2 | Relationship between the content of the saturated hydrocarbon and the viscosity (20°C) for the crude oil extracted from the Jimsar Sag.

of which four (#3, #9, #15, and #22) were also subjected to high-pressure mercury injection analysis. The experimental results are presented in **Appendix Tables A3**, **A4**, respectively.

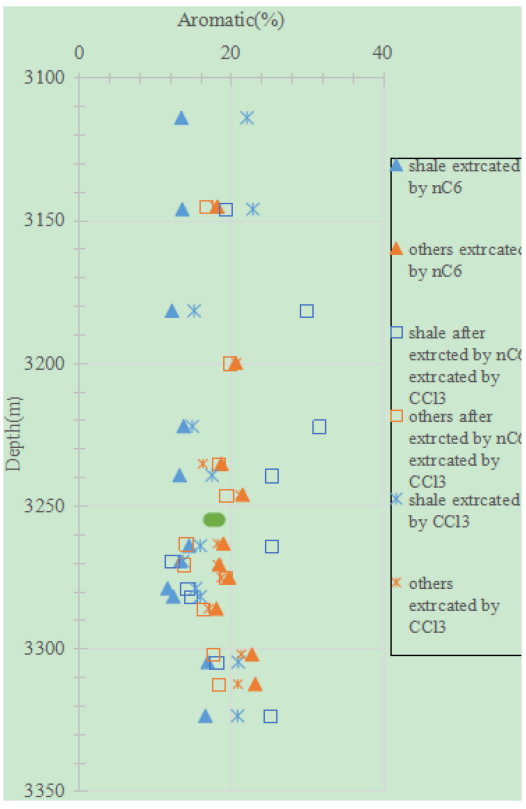

FIGURE 3 | Depth profile of the extract contents of the aromatic hydrocarbon from the mud shale versus the non-mud shale after different extraction treatments.

Extract Contents of the Component After Extraction

Saturated Hydrocarbon

The extract contents (as a percentage of the total extracted components; the same hereafter) of the saturated hydrocarbon were similar for the mud shale samples and the non-mud shale samples after extraction with nC_6. The extract contents of the saturated hydrocarbon from the samples of the oil-producing strata were similar to those of the crude oil samples (**Figure 1**). However, there was a significant difference in the extract contents of the saturated hydrocarbon for the two rock types after sequential extraction with nC_6 and $CHCl_3$. The mud shale samples had significantly smaller contents than the non-mud shale samples (**Figure 1**). For the oil-producing strata, the extract contents of the saturated hydrocarbon for the non-mud shale samples after sequential extraction with nC_6 + $CHCl_3$ were similar to those of the saturated hydrocarbon in crude oil samples, but the extract contents from the mud shale samples were significantly lower than those of the crude oil samples. The extract contents of the saturated hydrocarbon from the mud shale samples were lower than those from the non-mud shale samples after extraction with $CHCl_3$, which is similar to the case of the sequential extraction with nC_6 + $CHCl_3$. In other words, the mud shale was similar to the non-mud shale in terms of the extract contents of the saturated hydrocarbon after single-solvent extraction with $CHCl_3$ or after sequential extraction with nC_6 + $CHCl_3$. For the non-mud shale samples of the oil-producing strata, the extract contents of the saturated hydrocarbon were similar to those of the crude oil samples (**Figure 1**). However, the extract contents of the saturated hydrocarbon from the mud shale samples decreased in the order of single-solvent extraction with nC_6, single-solvent extraction with $CHCl_3$, and sequential extraction with nC_6 and $CHCl_3$. That is, the extract content gradually shifts toward the left along the abscissa in **Figure 1** when samples from the same sampling depth

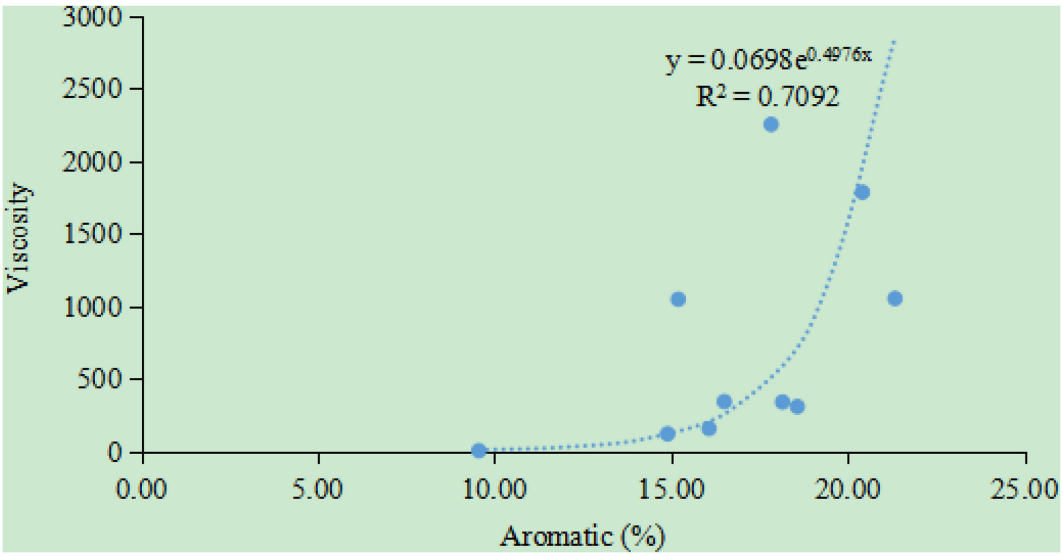

FIGURE 4 | Relationship between the content of the aromatic hydrocarbon and the viscosity (20°C) for crude oil extracted from the Jimsar Sag (the crude oil data were provided by the Xinjiang Oilfield Company of CNPC).

were separately subjected to the above-mentioned extraction treatments. This indicates that the extract contents of the saturated hydrocarbon from the mud shale samples are greatly dependent on the polarity of the organic solvent, with a higher polarity leading to a weaker extraction and thus a lower extract content. However, this pattern was not obvious for the non-mud shale samples.

Moreover, the higher the saturated hydrocarbon content, the lower the viscosity is (**Figure 2**), exhibiting an obvious negative correlation with a correlation coefficient R^2 of 0.86. Studies have shown that for crude oil, the higher the content of the saturated hydrocarbon, the lower the viscosity, and the easier it is to extract it from underground reservoirs (Boak and Kleinberg, 2020; Zhang et al., 2021).

Aromatic Hydrocarbon

The extract contents of the aromatic hydrocarbon from the mud shale samples after extraction with nC_6 were significantly lower than those from the non-mud shale samples (**Figure 3**). Moreover, the extract contents from the non-mud shale samples of the oil-producing strata were similar to those of the crude oil samples, but the extract contents from the mud shale samples from the same strata were obviously higher. However, the opposite patterns were observed for the case of the sequential extraction with nC_6 + $CHCl_3$. (1) The extract contents of the aromatic hydrocarbon from the mud shale samples after sequential extraction with nC_6 + $CHCl_3$ were significantly higher than those of from the non-mud shale samples (**Figure 3**). (2) For the oil-producing strata, the extract contents from the non-mud shale samples were lower than those of the crude oil samples, but the extract contents from the mud shale samples were significantly higher. For extraction with $CHCl_3$, the extract contents of the aromatic hydrocarbon from the mud shale samples versus the non-mud shale samples did not exhibit a clear trend, which is consistent with the results of other

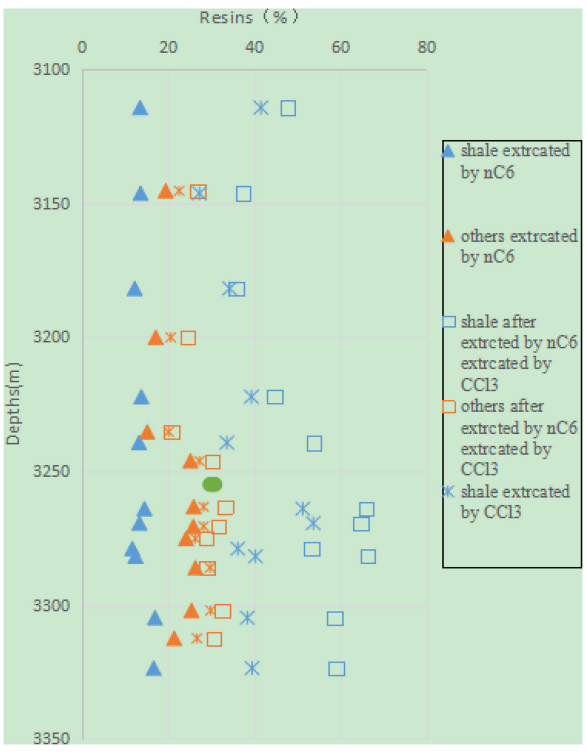

FIGURE 5 | Depth profile of the extract contents of the non-hydrocarbon from the mud shale versus the non-mud shale after different extraction treatments.

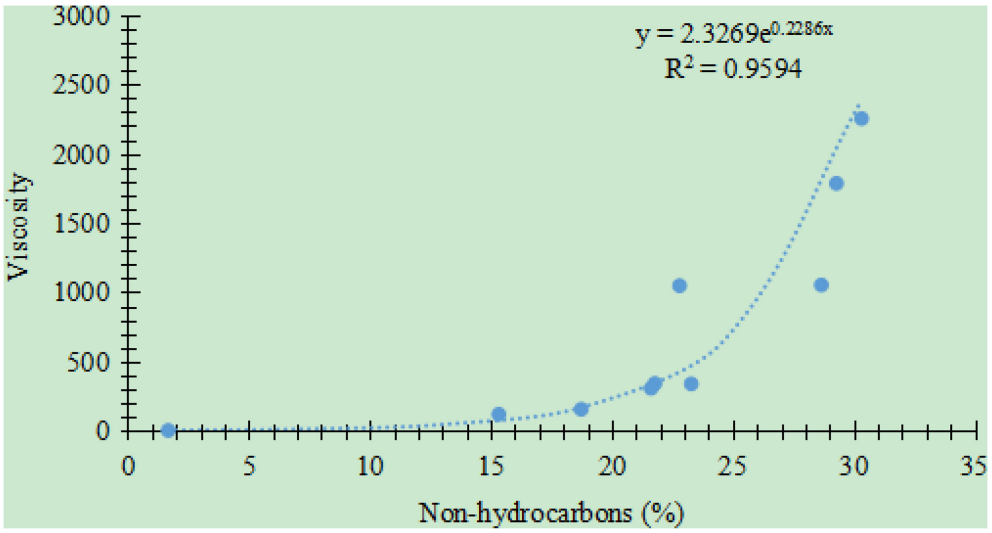

FIGURE 6 | Relationship between the content of the non-hydrocarbon and the viscosity (20°C) for crude oil extracted from the Jimsar Sag (the crude oil data were provided by the Xinjiang Oilfield Company of CNPC).

studies (Chishti and Williams, 1999; Jefimova et al., 2014; Fang et al., 2019).

For the mud shale, the extract contents of the aromatic hydrocarbon decreased in the order of $nC_6 + CHCl_3$, $CHCl_3$, and nC_6. This indicates that the aromatic hydrocarbon in the shale oil can be extracted by chloroform and n-hexane. For the non-mud shale, the extract contents obtained using the three extraction treatments did not vary significantly.

Moreover, the higher the aromatic content, the higher the viscosity of the crude oil, exhibiting an obvious positive correlation with an R^2 of 0.71 (**Figure 4**). For the crude oil, the higher the content of the aromatic hydrocarbon, the heavier the oil (i.e., the higher the viscosity), and the harder it is to extract it from underground reservoirs (Chen et al., 2010; Yu et al., 2018; Aily et al., 2019).

Non-hydrocarbon

For the non-hydrocarbon, its extract contents after extraction with nC_6 were significantly lower for the mud shale samples than for the non-mud shale samples (**Figure 5**). But the opposite was observed for the case of sequential extraction with $nC_6 + CHCl_3$. The extract contents of the non-hydrocarbon from the mud shale samples were higher than those from the non-mud shale samples. This pattern was also similarly observed for the case of extraction with $CHCl_3$. As is shown above, the extract contents of the non-hydrocarbon after extraction with $CHCl_3$ or $nC_6 + CHCl_3$ were higher for the mud shale samples than for the non-mud shale samples.

For a given sample, the extract contents decreased in the order of $nC_6 + CHCl_3$, $CHCl_3$, and nC_6. This suggests that the more polar the solvent, the higher the content of the extracted non-hydrocarbon.

Moreover, the higher the non-hydrocarbon content, the higher the viscosity of the crude oil, exhibiting an obvious positive correlation with an R^2 of 0.96 (**Figure 6**). This suggests that for crude oil, the higher the non-hydrocarbon content, the heavier the oil (i.e., the higher

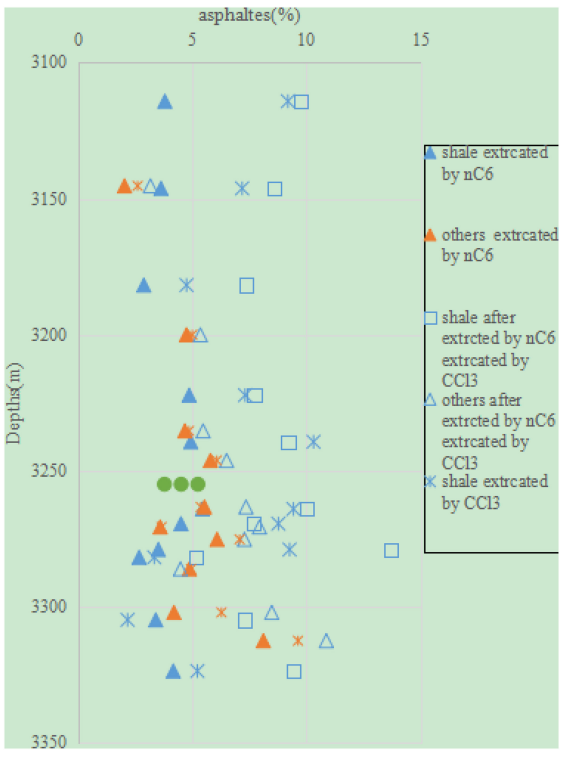

FIGURE 7 | Depth profile of the extract contents of the asphaltene from the mud shale versus the non-mud shale samples after different extraction treatments.

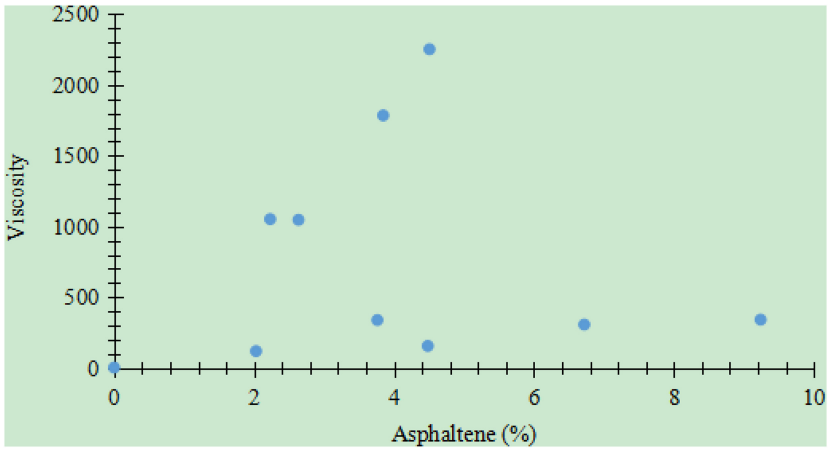

FIGURE 8 | Relationship between the content of the asphaltene and the viscosity (20°C) for crude oil extracted from the Jimsar Sag (the crude oil data were provided by the Xinjiang Oilfield Company of CNPC).

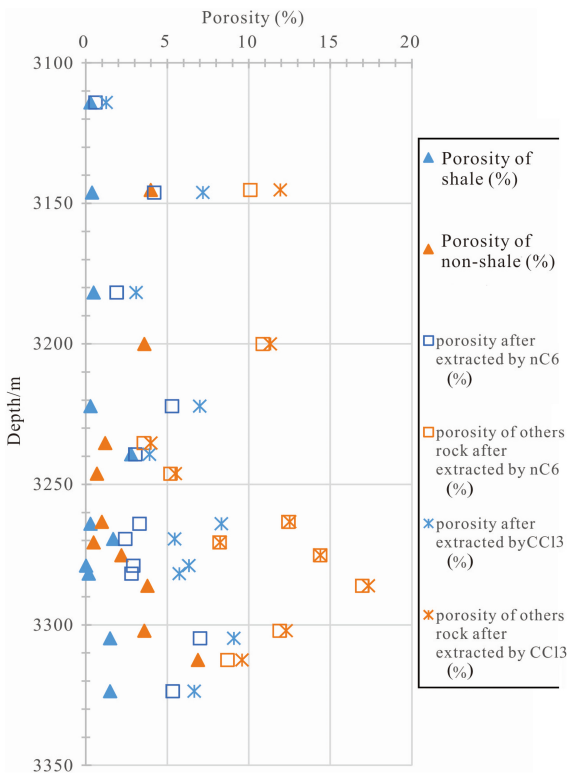

FIGURE 9 | Porosity of the mud shale samples versus the non-mud shale after extraction with nC_6 alone or with $CHCl_3$ alone.

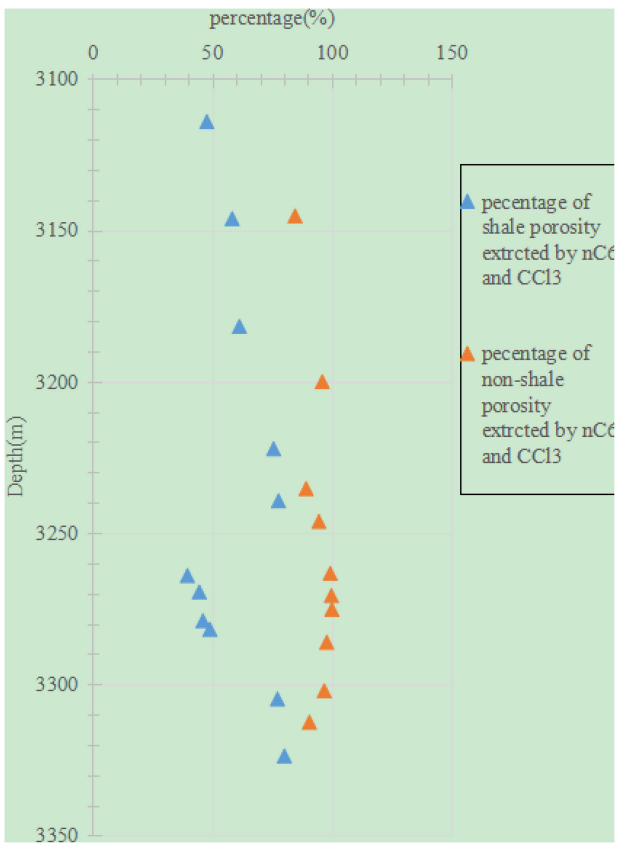

FIGURE 10 | Porosity of the mud shale samples versus the non-mud shale after sequential extraction with nC_6 + $CHCl_3$.

the viscosity), and the harder it is to extract in from underground reservoirs.

Asphaltene

For extraction with nC_6, the extract contents of the asphaltene from the mud shale samples versus the non-mud shale samples do not exhibit a clear trend. For extraction with nC_6 + $CHCl_3$, the extract contents were significantly higher for the mud shale samples than for the non-mud shale samples. For extraction with

$CHCl_3$, the extract contents were generally higher for the mud shale samples than for the non-mud shale samples (**Figure 7**).

For the mud shale samples, the extract contents of the asphaltene decreased in the order of $nC_6 + CHCl_3$, $CHCl_3$, and nC_6. This suggests that the higher the polarity of the organic solvent ($nC_6 + CHCl_3$), the higher the content of the extracted asphaltene. The lower the polarity of the organic solvent (nC_6), the smaller the content of the extracted asphaltene is. This pattern was also observed for the non-mud shale samples.

Moreover, there was no obvious correlation between the viscosity of the crude oil and the content of the asphaltene (**Figure 8**). The content of the asphaltene did not affect the viscosity of the crude oil.

Porosity After the Different Extraction Treatments

The original porosity of the non-mud shale samples were generally slightly higher than those of the mud shale samples. After single-solvent extraction with nC_6 or $CHCl_3$, the porosity of the non-mud shale was still higher than those of the mud shale (**Figure 9**). For the mud shale and non-mud shale samples, the porosity after extraction with nC_6 or $CHCl_3$ was higher than the original porosity. In particular, the porosity after extraction with $CHCl_3$ were higher than those after extraction with nC_6, and both values were higher than the original porosity. This shows that extraction with organic solvents increases the porosity of mud shale and non-mud shale. The higher the polarity, the larger the increase is. After sequential extraction with $nC_6 + CHCl_3$, the increase was more obvious for the non-mud shale samples than for the mud shale samples (**Figure 10**).

CONCLUSION

In this study, an experimental method for quantitative assessment of movable shale oil was established. The results revealed that the extract contents of the four components vary among the different extraction treatments and different lithology. The mud shale and non-mud shale exhibited similar extract contents of the saturated hydrocarbon after single-solvent extraction with $CHCl_3$ or sequential extraction with $nC_6 + CHCl_3$. For the aromatic hydrocarbon, the mud shale exhibited lower extract content than the non-mud shale after extraction with nC_6, but they exhibited higher extract content after extraction with $nC_6 + CHCl_3$. However, for extraction with $CHCl_3$, the extract contents of the aromatic hydrocarbon from the mud shale versus non-mud shale did not exhibit a clear trend. For the non-hydrocarbon, the mud shale exhibited lower extract content than the non-mud shale after single-solvent extraction with nC_6, but they exhibited higher extract content after single-solvent extraction with $CHCl_3$ or sequential extraction with $nC_6 + CHCl_3$. For the asphaltene, its content in the nC_6 extract did not exhibit a clear trend between the mud shale and the non-mud shale. In contrast, its extract content was higher for the mud shale than for the non-mud shale after extraction with $nC_6 + CHCl_3$ or with $CHCl_3$ alone. The viscosity of the crude oil exhibits a negative correlation with the saturated hydrocarbon, positive correlations with the aromatic hydrocarbon and the non-hydrocarbon, and no correlation with the asphaltene. The porosity after single-solvent extraction with nC_6 or $CHCl_3$ was higher than their original porosity. In particular, the porosity after extraction with $CHCl_3$ was higher than that after extraction with nC_6. There was correlation between the movable shale oil and lithology, with sandstone allowing for a higher fluid movability than mud shale and dolomite allowing for a higher fluid movability than siliceous rocks.

DATA AVAILABILITY STATEMENT

The original contributions presented in the study are included in the article/supplementary material, further inquiries can be directed to the corresponding author/s.

AUTHOR CONTRIBUTIONS

XL: conceptualization, methodology, investigation, and writing. ZZ: formal analysis, resources, data curation, and writing. LH: software, validation, project administration, and methodology. SL: software, project administration, and data validation. FS: data validation and analysis and software. LZ: data interpretation, draft, and approval. YZ: drawing of figures, data analysis, and references. All authors contributed to the article and approved the submitted version.

FUNDING

This study was funded by the PetroChina Co., Ltd. (Grant No. 2015D-4810-02; 2018ycq03). The funder was not involved in the study design, collection, analysis, interpretation of data, the writing of this article or the decision to submit it for publication.

ACKNOWLEDGMENTS

We sincerely thank Garcia for his continuous care and help. We also thank Wilson for reviewing our article. We benefit from Allen for providing polishing and editing services to our manuscript.

REFERENCES

Aily, M. E., Mansour, E. M., Desouky, S. M., and Helmi, M. E. (2019). Modeling viscosity of moderate and light dead oils in the presence of complex aromatic structure. *J. Pet. Sci. Eng.* 173, 426–433. doi: 10.1016/j.petrol.2018.10.024

Boak, J., and Kleinberg, R. (2020). *Future Energy*, 3rd Edn, Amsterdam: Elsevier Press.

Burnham, A. K. (2017). Porosity and permeability of Green River oil shale and their changes during retorting. *Fuel* 203, 208–213. doi: 10.1016/j.fuel.2017.04.119

Chen, Y. L., He, J., Wang, Y. P., and Li, P. (2010). GC-MS used in study on the mechanism of the viscosity reduction of heavy oil through aquathermolysis catalyzed by aromatic sulfonic $H_3PMo_{12}O_{40}$. *Energy* 35, 3454–3460. doi: 10.1016/j.energy.2010.04.041

Chishti, H. M., and Williams, P. T. (1999). Aromatic and hetero-aromatic compositional changes during catalytic hydrotreatment of shale oil. *Fuel* 78, 1805–1815. doi: 10.1016/s0016-2361(99)00089-7

Dong, T., and Harris, N. B. (2020). The effect of thermal maturity on porosity development in the Upper devonian –lower Mississippian Woodford Shale, Permian Basin, US: insights into the role of silica nanospheres and microcrystalline quartz on porosity preservation. *Intern. J. Coal Geol.* 217:103346. doi: 10.1016/j.coal.2019.103346

Fang, R. H., Littke, R., Zieger, L., Baniaasad, A., Li, M. J., and Schwarzbauer, J. (2019). Changes of composition and content of Tricyclic Terpane, Hopane, Sterane, and aromatic biomarkers throughout the oil window: a detailed study on maturity parameters of Lower Toarcian Posidonia Shale of the Hils Syncline, NW Germany. *Organ. Geochem.* 138:103928. doi: 10.1016/j.orggeochem.2019.103928

Gao, J., and Li, Z. X. (2018). Water saturation-driven evolution of helium permeability in Carboniferous shale from Qaidam Basin, China: an experimental study. *Mar. Petrol. Geol.* 96, 371–390. doi: 10.1016/j.marpetgeo.2018.05.028

Goodarzi, F. (2020). Comparison of the geochemistry of lacustrine oil shales of Mississippian age from Nova Scotia and New Brunswick, Canada. *Intern. J. Coal Geol.* 220:103398. doi: 10.1016/j.coal.2020.103398

Hou, L. H., Luo, X., Han, W. X., Lin, S. H., Pang, Z. L., and Liu, J. Z. (2020a). Geochemical evaluation of the hydrocarbon potential of shale oil and its correlation with different minerals-a case study of the TYP shale in the Songliao Basin, China. *Energy Fuels* 34, 11998–12009. doi: 10.1021/acs.energyfuels.0c01285

Hou, L. H., Ma, W. J., Luo, X., and Liu, J. Z. (2020b). Characteristics and quantitative models for hydrocarbon generation-retention-production of shale under ICP conditions: example from the Chang 7 member in the Ordos Basin. *Fuel* 279:118497. doi: 10.1016/j.fuel.2020.118497

Hou, L. H., Ma, W. J., Luo, X., Liu, J. Z., Lin, S. H., and Zhao, Z. Y. (2021). Hydrocarbon generation-retention-expulsion mechanism and shale oil producibility of the Permian lucaogou shale in the Junggar Basin as simulated by semi-open pyrolysis experiments. *Mar. Petrol. Geol.* 125:104880. doi: 10.1016/j.marpetgeo.2020.104880

Hu, S. Y., Zhao, W. Z., Hou, L. H., Yang, Z., Zhu, R. K., Wu, S. T., et al. (2020). Development potential and technical strategy of continental shale oil in China. *Pet. Explor. Dev.* 47, 877–887. doi: 10.1016/s1876-3804(20)60103-3

Jefimova, J., Irha, N., Reinik, J., Kirso, U., and Steinnes, E. (2014). Leaching of polycyclic aromatic hydrocarbons from oil shale processing waste deposit: a long-term field study. *Sci. Total Environ.* 481, 605–610. doi: 10.1016/j.scitotenv.2014.02.105

Kara, B., and Isik, V. (2021). Reservoir characteristics and unconventional oil potential of Silurian aged Dadaş shale in southeast Turkey. *J. Pet. Sci. Eng.* 200:108365. doi: 10.1016/j.petrol.2021.108365

Kim, M., and Shin, H. (2020). Numerical simulation of undulating shale breaking with steam-assisted gravity drainage (UB-SAGD) for the oil sands reservoir with a shale barrier. *J. Pet. Sci. Eng.* 195:107604. doi: 10.1016/j.petrol.2020.107604

Li, W. H., Lu, S. F., Xue, H. T., Zhang, P. F., and Hu, Y. (2015). Oil content in argillaceous dolomite from the Jianghan Basin, China: application of new grading evaluation criteria to study shale oil potential. *Fuel* 143, 424–429. doi: 10.1016/j.fuel.2014.11.080

Liu, B., Lv, Y. F., Zhao, R., Tu, X. X., Guo, X. B., and Shen, Y. (2012). Formation overpressure and shale oil enrichment in the shale system of Lucaogou formation, Malang Sag, Santanghu Basin, NW China. *Pet. Explor. Dev.* 39, 744–750. doi: 10.1016/s1876-3804(12)60099-8

Ma, W. J., Hou, L. H., Luo, X., Tao, S. Z., Guan, P., Liu, J. Z., et al. (2020). Role of bitumen and NSOs during the decomposition process of a lacustrine Type-II kerogen in semi-open pyrolysis system. *Fuel* 259:116211. doi: 10.1016/j.fuel.2019.116211

Solarin, S. A. (2020). The effects of shale oil production, capital and labour on economic growth in the United States: a maximum likelihood analysis of the resource curse hypothesis. *Resour. Policy* 68:101799. doi: 10.1016/j.resourpol.2020.101799

Tao, S., Wang, Y. B., Tang, D. Z., Wu, D. M., Xu, H., and He, W. (2012). Organic petrology of Fukang Permian Lucaogou formation oil Shales at the northern foot of Bogda Mountain, Junggar Basin, China. *Intern. J. Coal Geol.* 99, 27–34. doi: 10.1016/j.coal.2012.05.001

Xie, X. M., Borjigin, T., Zhang, Q. Z., Zhang, Z. R., Qin, J. Z., Bian, L. Z., et al. (2015). Intact microbial fossils in the Permian Lucaogou Formation oil shale, Junggar Basin, NW China. *Intern. J. Coal Geol.* 146, 166–178. doi: 10.1016/j.coal.2015.05.011

Yu, Z. S., Dai, M. Q., Huang, M. M., Fang, S. W., Xu, J. C., Lin, Y., et al. (2018). Catalytic characteristics of the fast pyrolysis of microalgae over oil shale: analytical Py-GC/MS study. *Renew. Energy* 125, 465–471. doi: 10.1016/j.renene.2018.02.136

Zhang, L. Y., Wu, K. L., Chen, Z. X., Li, J., Yu, X. R., Hui, G., et al. (2021). The increased viscosity effect for fracturing fluid imbibition in shale. *Chem. Eng. Sci.* 232:116352. doi: 10.1016/j.ces.2020.116352

Zhao, W. Z., Zhu, R. K., Hu, S. Y., Hou, L. H., and Wu, S. T. (2020). Accumulation contribution differences between lacustrine organic-rich shales and mudstones and their significance in shale oil evaluation. *Pet. Explor. Dev.* 47, 1160–1171. doi: 10.1016/s1876-3804(20)60126-x
doi: 10.1016/j.petrol.2020.107926

Conflict of Interest: All authors are affiliated with the company PetroChina Co., Ltd.

APPENDIX

TABLE A1 | Basic geochemical information for the samples.

Samples	Depth (m)	Lithology	Type	Initial				Extracted after trichloromethane				Minerals (%)						
				TOC (%)	S_1 (mg/g)	S_2 (mg/g)	Tmax (°C)	TOC (%)	S_1 (mg/g)	S_2 (mg/g)	Tmax (°C)	Quartz	Potash feldspar	Plagioclase	Calcite	Dolomite	Pyrite	Clay
#1	3114.17	Silty mudstone	Shale	7.93	0.57	48.71	445	7.50	0.30	21.57	439	40.2	0	42.1	0	3.1	0	14.6
#2	3145.29	Dolomite	Non-shale	0.94	6.18	6.49	435	0.08	0.05	1.04	437	11	0	22.5	0	66.5	0	0
#3	3146.2	Silt-bearing mudstone	Shale	5.34	0.31	27.88	441	4.89	0.15	25.99	441	27.5	13.4	23.2	6.6	15.1	0	14.2
#4	3181.77	Dolomitic mudstone	Shale	6.12	1.07	43.61	444	5.65	0.20	40.76	440	30.1	0	36.4	0	22.2	0	11.3
#5	3200.04	Lime siltstone	Non-shale	1.15	5.63	5.28	433	0.20	0.12	1.16	435	25.9	6.4	41.2	15.9	10.6	0	0
#6	3222.24	Lime mudstone	Shale	3.87	2.78	26.25	437	3.39	0.26	22.28	437	29.3	2.6	29.1	0	34.6	0	4.4
#7	3235.38	Dolomitic siltstone	Non-shale	1.72	5.28	8.10	437	0.77	0.11	4.47	442	34.8	3.4	25.2	0	36.6	0	0
#8	3239.41	Dolomitic mudstone	Shale	2.54	3.22	9.77	437	1.46	0.08	4.01	444	20.4	6.9	28.5	0.0	36.3	0.0	7.9
#9	3246.26	Muddy siltstone	Non-shale	0.23	0.93	0.85	437	0.24	0.09	0.55	439	29.6	11.8	42.6	12	4	0	0
#10	3263.36	Dolomitic siltstone	Non-shale	3.34	28.42	22.98	430	0.75	0.12	1.93	435	27.7	0	26.9	0	45.3	0	0
#11	3264.09	Dolomitic mudstone	Shale	2.87	0.58	12.83	439	2.27	0.04	12.26	439	34.4	0	37.1	0	21.1	0	7.4
#12	3269.5	Dolomitic mudstone	Shale	8.76	0.76	66.73	440	7.32	0.05	55.80	443	23.3	0.9	28.8	0.8	31.5	5.2	9.5
#13	3270.7	Dolomitic siltstone	Non-shale	2.48	24.88	23.42	437	0.60	0.09	2.07	437	22	1.4	27.3	0.2	44.4	0	4.7
#14	3275.25	Dolomitic siltstone	Non-shale	2.06	30.74	27.71	435	0.27	0.08	1.11	437	24.3	0	50.3	0	25.3	0	0
#15	3279.01	Dolomitic mudstone	Shale	8.10	2.77	94.24	441	7.99	0.21	58.84	444	25.9	0	18.5	6.6	49	0	0
#16	3281.87	Dolomitic mudstone	Shale	11.01	0.97	88.36	446	9.96	0.40	59.73	443	11.2	0.7	16.9	0.0	66.0	0.0	5.2
#17	3286.14	Dolomitic siltstone	Non-shale	3.73	37.33	24.95	435	0.20	0.07	1.31	434	24.5	8.6	42.8	0	24.1	0	0
#18	3302.13	Dolomitic siltstone	Non-shale	2.13	19.05	17.28	435	0.12	0.11	0.88	437	27	0	38.4	0	34.6	0	0
#19	3304.86	Dolomitic mudstone	Shale	5.65	10.55	31.40	440	3.64	0.18	11.61	440	22.1	2	18.9	0	56.9	0	0
#20	3312.54	Lime siltstone	Non-shale	1.69	16.23	12.86	430	0.08	0.10	0.79	433	13.1	5.2	49	19.9	12.7	0	0
#21	3323.67	Dolomitic mudstone	Shale	5.91	3.80	34.33	4380	4.45	0.20	28.45	436	21.3	0	16.2	12.9	49.6	0	0

TABLE A2 | Analysis results of the extracts after different extraction treatments.

Samples	nC_6				$nC_6 + CHCl_3$				$CHCl_3$				nC_6		$CHCl_3$	
	Saturated	Aromatic	Resin	Asphaltene	Saturated	Aromatic	Resin	Asphaltene	Saturated	Aromatic	Resin	Asphaltene	K (mD)	Φ (%)	K (mD)	Φ (%)
#1	58.05	23.65	13.51	3.79	23.24	19.24	47.79	9.73	27.10	22.14	41.58	9.19	0.0043	0.60	0.0077	1.26
#2	60.27	18.23	19.47	2.02	53.35	16.67	26.82	3.16	56.88	17.93	22.59	2.60	0.0085	10.10	0.0151	11.94
#3	57.00	25.75	13.63	3.63	24.09	29.89	37.42	8.60	42.59	22.91	27.31	7.18	0.0058	4.20	0.0067	7.20
#4	60.95	23.91	12.27	2.87	25.25	31.61	35.77	7.37	45.75	15.18	34.33	4.74	0.0085	1.90	0.0120	3.10
#5	57.46	20.65	17.16	4.74	50.37	19.85	24.43	5.35	53.60	20.76	20.65	5.00	0.0120	10.87	0.0180	11.33
#6	57.78	23.55	13.81	4.86	22.17	25.34	44.78	7.71	38.36	14.95	39.38	7.31	0.0042	5.29	0.0067	7.00
#7	61.38	18.77	15.18	4.67	55.49	18.31	20.73	5.47	58.67	16.32	20.16	4.85	0.0055	3.57	0.0141	4.00
#8	58.47	23.33	13.27	4.93	11.58	25.34	53.88	9.20	38.46	17.54	33.69	10.31	0.0006	3.05	0.0037	3.93
#9	47.43	21.56	25.22	5.79	43.82	19.36	30.32	6.50	45.43	21.22	27.28	6.07	0.0010	5.20	0.0044	5.50
#10	48.98	34.32	12.33	4.37	13.32	28.20	52.25	6.23	33.98	19.65	38.17	5.60	0.0280	1.79	0.0830	3.08
#11	49.45	19.04	25.98	5.53	45.38	14.04	33.23	7.35	48.06	18.28	28.29	5.37	0.0018	12.43	0.0069	12.52
#12	47.82	32.22	14.53	5.44	11.82	12.21	65.98	9.99	23.27	15.99	51.31	9.43	0.0005	3.30	0.0034	8.32
#13	47.35	34.78	13.37	4.50	13.32	14.25	64.77	7.66	23.78	13.70	53.75	8.77	0.0006	2.43	0.0034	5.46
#14	52.03	18.50	25.88	3.59	46.55	13.82	31.69	7.94	49.80	18.26	28.29	3.65	0.0012	8.22	0.0023	8.24
#15	49.96	19.77	24.19	6.08	44.67	19.33	28.72	7.28	47.79	18.78	26.36	7.07	0.0081	14.39	0.0085	14.40
#16	50.88	33.92	11.70	3.51	18.28	14.70	53.31	13.71	39.13	15.39	36.22	9.26	0.0039	2.92	0.0067	6.33
#17	56.44	28.44	12.44	2.67	10.34	18.10	66.38	5.17	40.35	15.99	40.33	3.33	0.0007	2.82	0.0017	5.74
#18	50.63	18.12	26.38	4.87	50.25	16.33	28.94	4.48	48.20	17.09	29.76	4.94	0.0191	16.97	0.0370	17.35
#19	47.55	22.79	25.47	4.19	41.33	17.63	32.56	8.48	44.41	21.39	29.92	6.27	0.0046	11.91	0.0069	12.30
#20	48.84	30.79	16.98	3.40	8.85	25.17	58.69	7.29	38.43	20.99	38.42	2.16	0.0029	7.02	0.0049	9.09
#21	47.23	23.22	21.44	8.11	40.22	18.35	30.56	10.87	42.69	20.93	26.75	9.63	0.0021	8.69	0.0024	9.60

TABLE A3 | NMR analysis results.

No.	Lithology	0.05–0.1 μm	0.1–0.5 μm	0.5–1.0 μm	>1.0 μm	>0.05 μm
#3	Silt-bearing mudstone	2.99	3.12	1.58	0.57	8.26
#9	Muddy siltstone	5.34	5.50	3.02	1.52	15.37
#15	Dolomitic mudstone	4.20	26.08	22.47	15.75	68.50
#16	Dolomitic mudstone	5.81	7.61	10.96	26.70	51.09
#22	Dolomitic mudstone	3.00	5.49	3.65	9.87	22.02

TABLE A4 | High-pressure mercury injection results.

Samples	Lithology	>0.0037 μm	>0.018 μm	>0.048 μm	0.0037–0.018 μm	0.018–0.048 μm	0.048–0.133 μm	0.133–0.735 μm	0.735–0.942 μm	>0.942 μm
#3	Silt-bearing mudstone	60.69	9.629	4.282	51.061	5.347	3.223	1.059	0	0
#9	Muddy siltstone	80.74	67.27	49.71	13.47	17.56	33.64	16.055	0.015	0
#15	Dolomitic mudstone	81.91	80.84	77.04	1.07	3.8	37.75	39.29	13.437	9.88
#22	Dolomitic mudstone	85.75	14.81	3.358	70.94	11.452	3.358			